**P5R.7**

# PHYSICAL VALIDATION OF TRMM RAINFALL PRODUCTS USING A RADIATIVE TRANSFER MODEL

Shoichi Shige*, Hiroshi Sasaki and Ken'ichi Okamoto
Department of Space Engineering, Osaka Prefecture University, Osaka, Japan

## 1. INTRODUCTION

The Tropical Rainfall Measuring Mission (TRMM) satellite has been in operation for more than 7 years and providing distribution of rainfall throughout the Tropics using microwave observation from the Precipitation Radar (PR) and the TRMM Microwave Imager (TMI). PR, the first space-borne precipitation radar, provides height information based upon the time delay of the precipitation-backscattered return power, and has enabled us to directly obtain vertical profiles of precipitation over the global Tropics (Okamoto 2003). On the other hand, the TMI measures radiances that are the end product of the integrated effects of electromagnetic absorption/emission and scattering through a precipitating cloud along the sensor viewpath. Although differences in global averaged rainfall between the two sensors have been reducing from Version 4 to Version 5, a comparisons of tropical mean rainfall time series indicates that there are still large discrepancies in the 1998 El Nino-Southern Oscillation (ENSO) event (Robertson et al., 2003).

Several improvements have been implemented to create the most recent algorithm, the TRMM Version 6 algorithms. Preliminary indications are that the overall bias is being drastically reduced in version 6 of the products, but certain evidences to support the claim that the TRMM version-6 rain estimates are better than version-5 estimates has not yet be obtained. The most common method of satellite-retrieved rain estimates is to directly compare to ground validation measurements (ground truth) derived from rain gauge networks, ground weather radar, or a combination of the two. However, it has pr oven to be extremely difficult to make accurate ground-based measurement of precipitation. Moreover, the sparse nature of ground based validation campaigns does not provide sufficient information about changing cloud characteristics leading to algorithm errors.

In this paper, we validate TRMM version-5 and -6 rain estimates using a radiative transfer model. Comparisons between TMI-observed brightness temperatures and those simulated from PR2A25 and TMI2A12 rain profiles are performed for ITCZ rain systems during the 1998 El Nino event.

*Corresponding author address: Dr. Shoichi Shige, Department of Space Engineering, Osaka Prefecture University, 1-1 Gakuen-cho, Sakai, Osaka, 599-8531 Japan; e-mail: shige@aero.osakafu-u.ac.jp

## 2. TRMM RAINFALL PRODUCTS

The basis of TMI 2A12 algorithm is the estimated expected value or "Bayesian" calculation, in which retrieved precipitation are constructed from those cloud-resolving model (CRM)-generated profiles that are radiatively consistent with the observation (Kummerow and Coauthors, 2001). The improvements have been made to the CRMs that make up the a-priori database. In addition to using new simulations, the version 6 also explicitly includes melting layer model developed by Olson et al. (2001). On the other hand, PR 2A25 algorithm uses a "hybrid" of the Hitschfeld-Bordan method and the surface reference technique (Iguchi et al., 2000). Attenuation by cloud water, water vapor and O2 is taken into accounts by the version 6.

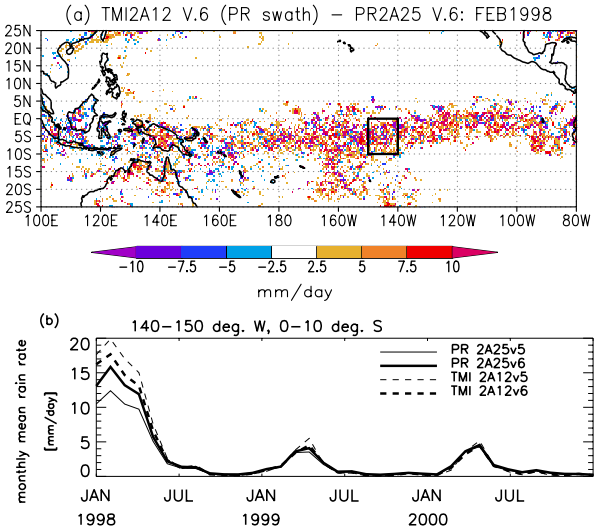


Figure 1: (a) Differences of rainfall estimates (mm day$^{-1}$) between TMI2A12 Version 6 and PR2A25 Version 6 for February of 1998; (b) Time series of monthly mean rainfall estimates (mm day$^{-1}$) from TMI and PR for the selected area extending from 0$^o$ to 10$^o$S latitude and from 140$^o$ to 150$^o$E longitude indicated by a box in (a). Only TMI data matched within PR swath are used.

Figure 1a indicates that PR Version 6-derived rain-

fall is still smaller than rainfall estimated by TMI Version 6 over a well-defined ITCZ (associated with heavy precipitation) which is present in the central and eastern Pacific between the equator and 10$^o$S. It is nevertheless obvious from Fig. 1b that the difference between TMI and PR estimates for February 1998 is drastically narrowing in Version 6 (1.8 mm day$^{-1}$, or 11 %) compared with Version 5 (7.5 mm day$^{-1}$, or 46 %) for the area from 0$^o$ to 10$^o$S latitude and from 140$^o$ to 150$^o$E longtitude where larger differences are found in Fig. 1a.

## 3. APPROACH

In this study, we investigate the consistency in observed and simulated brightness temperature at 10.65 GHz channels ($\sim$2.8 cm), which provide total liquid water path estimates since most rain drops are Rayleigh with respect to X-band wavelength. Here, the simulated brightness temperature are derived from not only PR2A25 precipitation profiles but also TMI2A12 ones. One might consider that the simulated brightness temperature from TMI2A12 precipitation profiles should be identical to the observed one from which TMI2A12 precipitation profiles are derived. This may be true for algorithms which iteratively modify the profiles to minimize the differences between observed and simulated rightness temperatures (e.g. Smith et al. 1994), but not necessarily for TMI2A12 algorithm based on the Bayesian calculation.

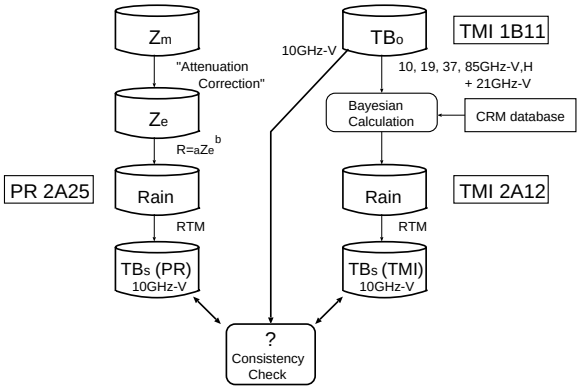


Figure 2: Diagram showing the procedure for validating the TRMM rainfall products. The "?" means to compare brightness temperature (TB) simulated from the TRMM rainfall products with the observed TB from TMI1B11.

The radiative transfer model (RTM) developed by Liu (1998) is used to calculate brightness temperatures. The upwelling microwave radiances over ocean depend on the sea surface characteristics and atmospheric constitutes. In this study, the sea surface temperature retrieved from TMI brightness temperature at 10.65 GHz by Wentz et al. (2000) is used. The salinity is set to a constant value of 35000 ppm. Mean atmospheric temperature and relative humidity profiles, and surface winds for the selected region from the 6-hourly ERA40 reanalysis data with minimum time difference with the TRMM observations are employed. ERA40 reanalysis is a repeat reanalysis performed by the European Center for Medium-Range Weather Forecasts (ECMWF). The slant-path approximation in which the actual three dimensional structure of the cloud is taken into account is used, following Bauer et al. (1998). The antenna pattern for 10.65 GHz is approximated by a Gaussian weighting function with the same 3-dB beamwidth as the actual antenna pattern.

For PR data, we used two DSD models of a gamma distribution corresponding to convective and stratiform rain assumed in PR algorithm (Kozu et al., 1999). A change in the DSD due to the "alpha-adjustment method" accommodating the SRT of PIA is also taken into account. For TMI data, we used Marshall and Palmer (1948) distribution assumed in the Goddard Cumulus Ensemble (GCE) model which is one of CRMs that make up the TMI2A12 database..

## 4. RESULTS AND DISCUSSIONS

### *4.1. Consistency check*

The procedures described in the previous section are applied to 6 months of TRMM data, from January to June 1998, in a region from 140$^o$ to 150$^o$E longitude. There are 132 TRMM orbits with TMI footprints of which 80% are coverd with PR rain pixels in this datasets.

Frequency plots of simulated brightness for 10 GHz-V from PR2A25 rain profiles, as a function of TMI1B11 observed brightness temperature for 10 GHz-V are presented in Fig. 3a,b for versions 5 and 6. Only the TMI footprint of which 80% are coverd with PR rain pixels are shown. $TB_s$ from PR2A25 V5 is much smaller than $TB_o$, especially for the higher range (i.e. heavy rainfall). The difference between $TB_s$ from PR2A25 V5 and $TB_o$ is about 20 K for $TB_o$ of 240 K. Olson et al. (2001) reported that at TMI resolution, the maximum radiance increase due to the inclusion of a melting-layer is 16 K at 10.65 GHz. Thus, the difference between $TB_s$ from PR2A25 V5 and $TB_o$ is due to PR algorithms rather than the impact of melting on radiances that are not considered in the calculations. This is consistent with Masunaga et al. (2002) who suggested that PR measurements are liable to suffer from ambiguity in the attenuation correction in heavy precipitation around the tropical rainfall maximum. $TB_s$ from PR2A25 V6 is higher than that from PR2A25 V5, and exhibits better agreement with $TB_o$, especially for higher values (associ-

ated heavy rainfall). This is probably explained by the fact that the attenuation due to cloud water that increases as rainfall rate is taken into account in the Version 6. Also, the spread in $TB_s$ from PR2A25 V6 is reduced than that from PR2A25 V5.These results indicates the improvement of PR2A25 estimates from Version 5 to Version 6. It is nevertheless obvious that $TB_s$ from PR2A25 V6 is too low. If the effects of cloud water and melting layer that increase brightness temperature are taken into account in the calculation, the better agreement between $TB_s$ from PR2A25 V6 and $TB_o$ may be achieved.

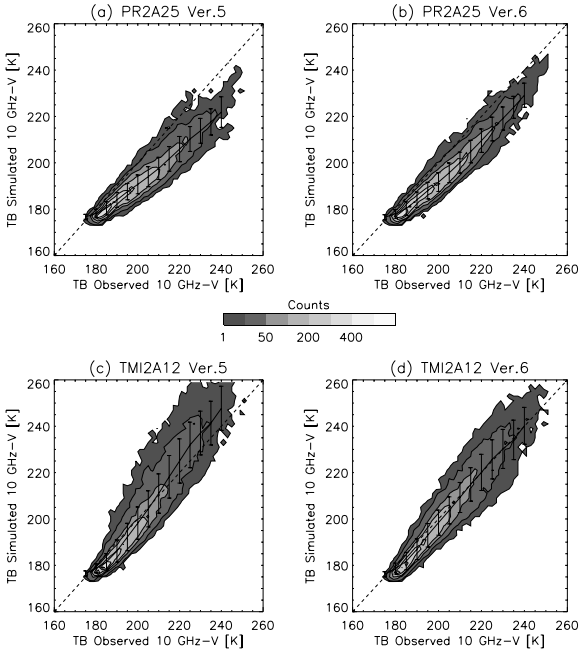


Figure 3: Frequency plots of simulated brightness temperature for 10 GHz-V, as a function of TMI1B11 observed brightness temperature for 10 GHz-V. A dashed lines indicating “perfect” agreement is indicated for reference.

Although $TB_s$ from TMI 2A12 V6 also exhibit better agreement with $TB_o$ than that from TMI2A12 V5 does, there is an excess of $TB_s$ from TMI 2A12 V6 over $TB_o$, especially for the higher range (Fig. 3c,d). Contrary to PR, the agreement between $TB_s$ from TMI2A12 V6 and $TB_o$ decreases, if the effects of cloud water and melting layer are taken into account in the calculation. $TB_s$ from TMI2A12 V6 exhibit more scatter against higher $TB_o$ than that from PR2A25 V6, although $TB_o$ is used in TMI rain retrieval and is not used in PR rain retrieval.

Cold brightness temperature at 85-GHz channels, which are mainly sensitive to ice scattering, play a significant role in matching ice phase hydrometeor profiles in the CRM database, thus, affecting the rainfall retrievals. Frequency plots of simulated brightness for 10.65 GHz-V from PR2A25 and TMI2A12 rain profiles, as a function of TMI1B11 observed brightness temperature for 85 GHz-V are presented in Fig. 3. The lack of $TB_s$ from PR V5 and V6 does not depends on 85-GHz brightness temperature. On the other hand, the excesses of $TB_s$ from TMI2A12 V5 over $TB_o$ rapidly increase as 85-GHz brightness temperature decreases. This is consistent with Kim et al. (2004) who suggested that the TMI2A12 V5 overestimated surface rainfall with respect to the KR because of strong ice scattering (85 GHz), which is not strongly correlated to surface rainfall. The TMI2A12 V6 have a much better performance than the TMI2A12 V5 because the database is updated, but the excesses of $TB_s$ from TMI2A12 V6 over $TB_o$ still depends on 85-GHz brightness temperature. Results suggest that efforts to improve the data base will be required.

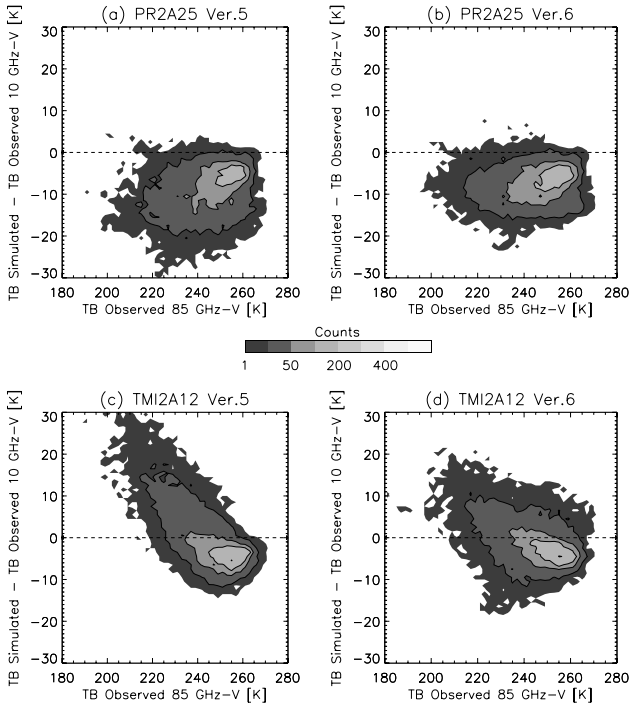


Figure 4: Frequency plots of differences between TMI observed brightness temperature for 10 GHz-V and simulated brightness temperature for 10 GHz-V, as a function of TMI observed brightness temperature for 85 GHz-V.

## 5. SUMMARY

The difference between TMI and PR estimates is drastically narrowing in Version 6 compared with Version 5. However, certain evidences to support the claim that the TRMM version-6 rain estimates are better than version-5 estimates has not yet be obtained. In this study, consistency between TMI-observed brightness temperatures and those simulated from PR2A25 and TMI2A12 rain profiles are

investigated for ITCZ rain systems during the 1998 ENSO event, using a radiative transfer model. We focus on brightness temperature at 10.65 GHz channels which provide total liquid water path estimates.

The better agreement between the observed and simulated brightness temperatures is obtained for PR 2A25 and TMI 2A12 version 6 than those for version 5. Simulated brightness temperature ($TB_s$) from PR2A25 V6 is higher than that from PR2A25 V5, and exhibits better agreement with observed brightness temperature ($TB_o$), especially for higher values (associated heavy rainfall). This is probably explained by the fact that the attenuation due to cloud water that increases as rainfall rate is taken into account in the Version 6. It is nevertheless obvious that $TB_s$ from PR2A25 V6 is low. If the effects of cloud water and melting layer that increase brightness temperature are taken into account in the calculation, the better agreement between $TB_s$ from PR2A25 V6 and $TB_o$ may be achieved. Although $TB_s$ from TMI 2A12 V6 also exhibit better agreement with $TB_o$ than that from TMI2A12 V5 does, there is an excess of $TB_s$ from TMI 2A12 V6 over $TB_o$, especially for the higher range. The excesses of $TB_s$ from TMI2A12 V6 over $TB_o$ are due to strong ice scattering (85-GHz), which is not strongly correlated to surface rainfall. These results suggest that efforts to improve both PR 2A25 and TMI 1B11 will be required.

**Acknowledgement** This study is supported by the fund of Japan Science and Technology Corporation - Core Research for Evolution Science and Technology (CREST). We wish to thank Prof. G. Liu of Florida State University for providing his radiative transfer model. We also thank Dr. K. Aonashi of Meteorological Research Institute for his kind guidance on using the radiative transfer model. Discussions with Drs. T. Iguchi, N. Takahashi of NICT and Prof. T. Kozu of Shimane University were appreciated. The TRMM products were provided by Japan Aerospace Exploration Agency (JAXA). ERA40 data was provided from the European Center for Medium-range Weather Forecasts., and SST products from TMI were obtained from Remote Sensing Systems.

## REFERENCES

Bauer, P., L. Schanz, and L. Roberti: 1998, Correction of three-dimensional effects for passive microwave remote sensing of convective clouds. *J. Appl. Meteor.*, **37**, 1619–1632.

Iguchi, T., T. Kozu, R. Meneghini, J. Awaka, and K. Okamoto: 2000, Rain-profiling algorithm for the TRMM precipitation radar. *J. Appl. Meteor.*, **39**, 2038–2052.

Kim, M.-J., J. A. Weinman, and R. A. Houze Jr.: 2004, Validation of maritime rainfall retrievals from the TRMM microwave radiometer. *J. Appl. Meteor.*, **43**, 847–859.

Kozu, T., T. Iguchi, K. Shimizu, and N. Kawagishi: 1999, Estimation of rain drop size distribution parameters using statistical relations between multiparameter rainfall remote sensing data. *Preprints, 29th Int. Conf. on Radar Meteorology*, Amer. Meteor. Soc., Montreal, Quebec, Canada, 689–692.

Kummerow, C. and Coauthors: 2001, The evolution of the Goddard profiling algorithm (GPROF) for rainfall estimation from passive microwave sensors. *J. Appl. Meteor.*, **40**, 1801–1820.

Liu, G.: 1998, A fast and accurate model for microwave radiance calculations. *J. Meteor. Soc. Japan*, **76**, 335–343.

Marshall, J. S. and W. M. Palmer: 1948, The distribution of raindrops with size. *J. Atmos. Sci.*, **5**, 165–166.

Masunaga, H., T. Iguchi, R. Oki, and M. Kachi: 2002, Comparison of rainfall products derived from TRMM microwave imager and precipitation radar. *J. Appl. Meteor.*, **41**, 849–862.

Okamoto, K.: 2003, A short history of the TRMM precipitation radar. *Cloud Systems, Hurricanes and The Tropical Rainfall Measurement Mission (TRMM): A Tribute to Dr. Joanne Simpson*, Meteor. Monogr, No. 51, Amer. Meteor. Soc., 187–195.

Olson, W. S., P. Bauer, C. D. Kummerow, Y. Hong, and W.-K. Tao: 2001, A melting-layer model for passive/active microwave remote sensing applications. Part II: Simulation of TRMM observations. *J. Appl. Meteor.*, **40**, 1164–1179.

Robertson, F. R., D. E. Fitzjarrald, and C. D. Kummerow: 2003, Effects of uncertainty in TRMM precipitation radar path integrated attenuation on interannual variations of tropical oceanic rainfall. *Geophys. Res. Lett.*, **30**, 1180, doi:10.1029/2002GL016416.

Smith, E. A., X. Xiang, A. Mugnai, and G. J. Tripoli: 1994, Design of an inversion-based precipitation profile retrieval algorithm using an explicit cloud model for initial guess microphysics. *Meteor. Atmos. Phys.*, **54**, 53–78.

Wentz, F. J., C. Gentemann, D. Smith, and D. Chelton: 2000, Satellite measurements of sea surface temperature through clouds. *Science*, **288**, 847–850.